Arch. Metall. Mater. **69** (2024), 2, 717-721

DOI: https://doi.org/10.24425/amm.2024.149802

R. GRZEJDA[1*], K. KWIATKOWSKI[1]

MODELLING OF MULTI-BOLTED SYSTEMS AT THE PRETENSION STAGE – PART 1: MECHANICAL CHARACTERISTICS OF THE CONTACT BETWEEN THE JOINED ELEMENTS

The subject of the paper is the modelling of multi-bolted connections that are at the pretensioning stage. Taking a systematic approach to the modelling issue, the connection was treated as a composite of four subsystems: a bolt set, a pair of joined elements and a contact layer between them. The first part of the paper describes experimental studies to determine the contact stiffness of a pair of elements separated from an exemplary asymmetric multi-bolted connection. The normal loading and unloading direction of the contact joint was considered. The tests were performed with the use of an INSTRON 8850 servo-hydraulic testing machine equipped with an extensometer. A normal stiffness characteristic in the form of an exponential function was proposed for the tested contact joint. It will be applied in the second part of the paper, in which finite element modelling of the multi-bolted connection will be presented.

Keywords: multi-bolted connection; systemic approach; contact joint; pretension stage; normal direction

1. Introduction

The proper operation of multi-bolted connections is conditioned by the appropriate stiffness of the contact joints present in these connections. Machine elements forming multi-bolted structures are most often joined on mechanically processed surfaces [1]. Their connection takes place not on the entire contact surface, but on a small part of it, depending on the surface texture, i.e. their roughness or waviness [2-4]. This can be even more evident in the case of joining elements produced by additive manufacturing [5,6]. Any unevenness on the contact surface affects the stiffness of the contact joint and the stiffness of the whole assembled structure. In the general case, when a multi-bolted connection is pretensioned and then loaded with an arbitrarily directed external load [7,8], this stiffness is influenced by physical phenomena occurring between the joined elements in the normal and tangential directions [9]. In engineering calculations, the description of these phenomena is usually reduced to including only constant coefficients of normal and tangential stiffness and friction in the contact model [10-13]. Then, these values remain constant over time on the entire contact surface of the joined elements. In fact, experimental validation of contact models outlines that this simplified modelling approach leads to the necessity to estimate the stiffness of the contact model in order to obtain the convergence of the results of calculations and experimental tests [14].

The phenomena at the contact of the joined elements in the case of small values of pressures and deformations, for which the contact layer shows high plasticity, can be described by non-linear relationships between the normal displacements of the points of this layer and the normal pressure and between the tangential displacements and the shear pressure [9,15]. In order to formalise the description of these phenomena, it is necessary to adopt an appropriate model of the rough surface of the interacting bodies and their contact. For this purpose, both analytical [16-18] and experimental [19-21] approaches are used.

Since analytical studies usually lead to very complex formulas describing the mechanical properties of the contact, in this paper it was decided to use experimental relationships for this purpose. The scope of the paper covers the pretensioning of the selected multi-bolted connection, i.e. the normal load direction of the contact of the joined elements. In this case, the contact features can be represented by an exponential function, as in [22-24]. This function can then be incorporated into the modelling of the contact in accordance with the concept of the so-called conventional third-body in the form of a thin layer [25].

The application of the third-body idea is easy to implement in finite element modelling (FE-modelling). By knowing the

[1] WEST POMERANIAN UNIVERSITY OF TECHNOLOGY IN SZCZECIN, FACULTY OF MECHANICAL ENGINEERING AND MECHATRONICS, 19 PIASTÓW AV., 70-310 SZCZECIN, POLAND

* Corresponding author: rafal.grzejda@zut.edu.pl

actual normal stiffness characteristics of a given contact, it can be taken into account independently for each of the FEs in the contact layer. More precisely, each of these elements, depending on the given loading situation, can have a different value of the normal stiffness coefficient, which is unattainable in the case of traditional contact modelling using commercial finite element method (FEM) programs.

Authors modelling contact joints most often use FEs with typical settings, according to which it is only possible to insert constant values of the normal and tangential contact stiffness into the model. Jaszak [26] and Jaszak et al. [27] conducted numerical analyses to determine the contact pressure on the contact surface between a serrated or flat gasket and a flange in the pipe connection. They used TARGET 170 and CONTA 174 surface-to-surface contact elements available in ANSYS software with standard settings. The same type of FEs and the same method of modelling contact joints have been applied, inter alia, in [28-31]. Authors using another popular commercial FEM software, ABAQUS, often assume contact properties as 'hard' contact in the normal direction without friction [32] or with friction [33]. Similarly, the same is true for the next FEM software, Midas NFX. In this case also, the constant normal and tangential stiffness coefficients as well as the friction coefficient are inserted [34,35]. In some papers, the stiffness of the contact layer is not mentioned in detail in the modelling. An information is then provided that the contact has been modelled in a standard way in the respective software [36-39].

Against the background of the above literature review, the idea of independently assigning to each contact layer element a stiffness coefficient depending on a given contact joint load is new. In order to take advantage of this idea, it is necessary to investigate the actual characteristics of a given contact joint. The procedure for determining such characteristics using the example of a contact joint separated from a multi-bolted connection, the experimental studies of which are described in [40,41], is presented in this paper.

By adopting a systemic approach to the modelling of multi-bolted connections [24], the modelling of the contacts occurring in them can be considered as a separate task. The idea of a third-body, mentioned above, is then useful and can be applied to the modelling of the contact joint. It can be inserted between models of the joined elements and then assigned experimentally determined mechanical properties [23]. This idea will be applied in the second part of the presented paper.

2. Experimental research of the contact of multi-bolted connection elements

The subject of the research is the contact joint between the elements joined in a multi-bolted connection, shown in Fig. 1. The connection is made by means of seven M10´1.25 fasteners (Fig. 1b). After machining, the bolts and nuts have been tempered to achieve the characteristics for the class of mechanical property 8.8 and 8, respectively.

The tested joint consists of two 28 mm thick plates made of S355J2 (1.0577) steel. Prior to testing, the contact surfaces were machined on a grinding machine. The shape of the contact surface is shown in Fig. 1d. It fits into a circle with a diameter of 175 mm. The size of this area was equal to 89.2×10^2 mm^2 and did not exceed the maximum pressure limit for S355J2 (1.0577) steel. The shape of the contact surface was defined as irregular in order to be able to create a universal FE-based model of the contact joint at a later step.

The contact joint of the plates was tested on an INSTRON 8850 testing machine. The joint loading was carried out in the direction normal to the contact surface, and the relative displacements of the joined plates were measured in two ways: by measuring the displacement of the testing machine heads using the machine software, and separately by means of an INSTRON extensometer (Fig. 2). The measuring base for the extensometer was set at 25 mm.

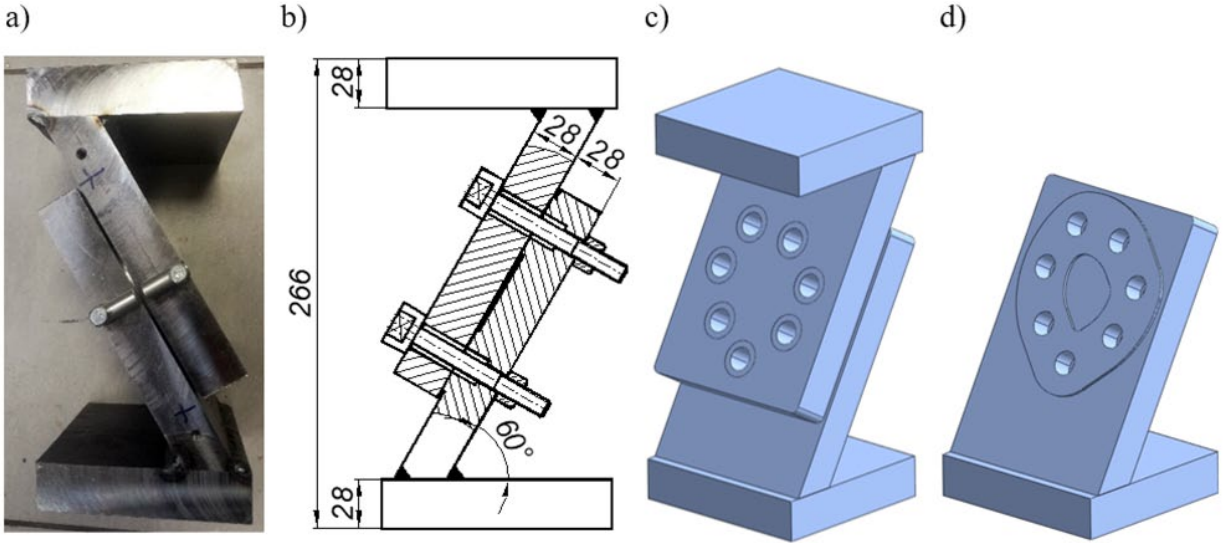

Fig. 1. Tested contact joint as a subsystem of a multi-bolted connection: a) general view, b) main dimensions of the connection, c), model, d) shape of the contact surface

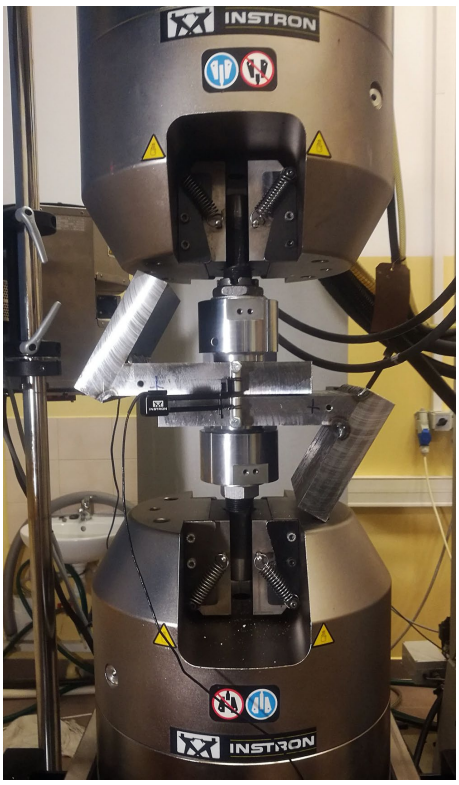

Fig. 2. Tested contact joint mounted on a testing machine

The testing machine control allows simultaneous loading of the joints under test and measurement of the displacements occurring in them. This makes it possible to independently generate both force vs. time and displacement vs. time diagrams.

The testing of the contact of multi-bolted connection elements was divided into two phases. In the first, the stiffness characteristics of the testing machine, understood as the contact stiffness characteristics of the compressed heads, were determined.

The time-varying loading of the head contact joint followed the characteristics shown in Fig. 3. Such a force curve was adopted in order to progressively load the tested joint and to be able to record the normal joint characteristics for the last unloading cycle in a later test phase, according to the Oliver-Pharr method [42]. Fig. 4 shows the head contact stiffness characteristics obtained as a result of the first phase tests.

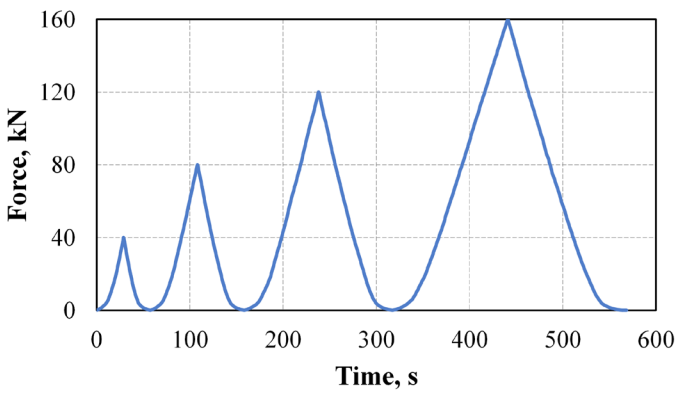

Fig. 3. Course of the force loading the contact joint of the heads

In the second phase of the research, the plate joint was set between the heads of the testing machine. As before, the joint was loaded with a time-varying force in the same force range, but over a shorter period of time. The loading duration of the heads alone and the heads-plates set had no effect on the resulting contact stiffness characteristics. Thus, after the first phase of testing, it was decided to reduce the loading duration while maintaining the range of variation for the loading force. The course of the loading force in this case is shown in Fig. 5.

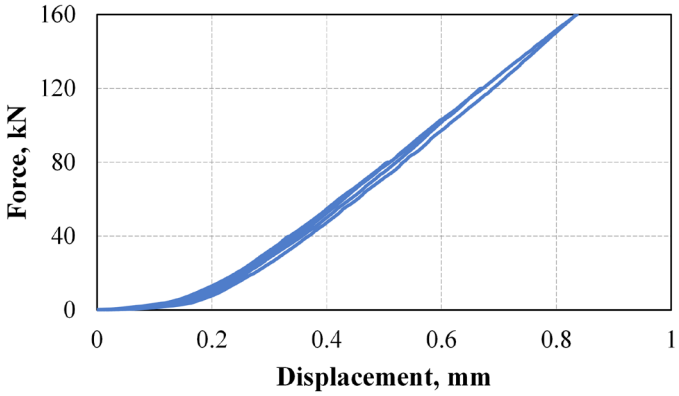

Fig. 4. Contact stiffness characteristics of the testing machine heads

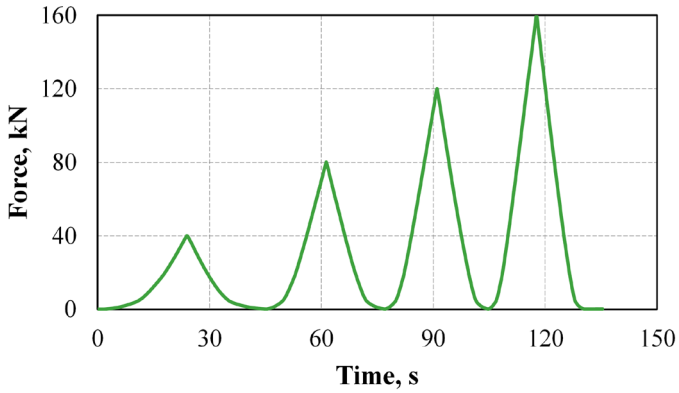

Fig. 5. Course of the force loading the contact joint of the plates and heads

Fig. 6 shows the contact stiffness characteristics of the plates and heads obtained as a result of the second phase tests.

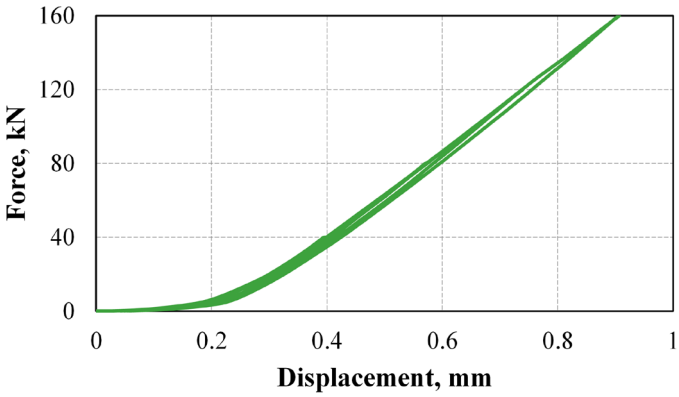

Fig. 6. Contact stiffness characteristics of the joint of the plates and heads

3. Normal contact characteristics of multi-bolted connection elements

In line with the previously mentioned principle, the characteristics of the tested plate contact joint was determined for the last cycle of unloading the joint. It can be assumed that then the final fit of the joined surfaces has taken place. Thus, when determining the stiffness characteristics based only on the unloading curve, the influence of plastic deformations between the joined elements is then neglected [42]. The normal characteristics identified in this way can be implemented in the contact element model, which is schematically shown in Fig. 7 [24].

By subtracting the displacements of the machine head joint from the displacements of the entire heads-plates system, the displacements in the contact layer between the joined plates can be obtained. Referring these to the force loading the joint, the characteristics of its normal stiffness can be drawn. Both stiffness characteristics for the last unloading cycle are shown in Fig. 8.

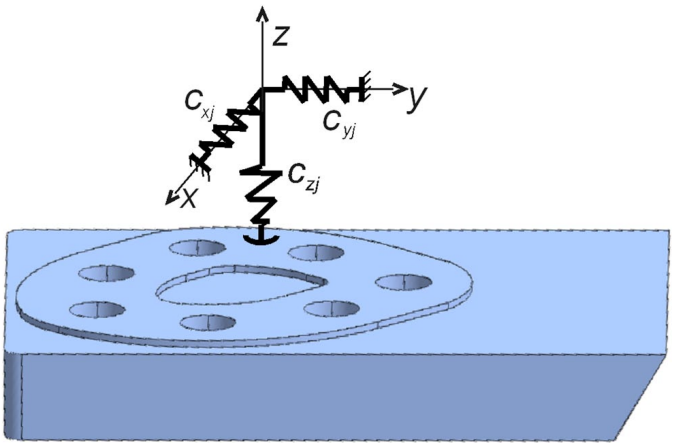

Fig. 7. Bottom plate with single spring model of the contact layer

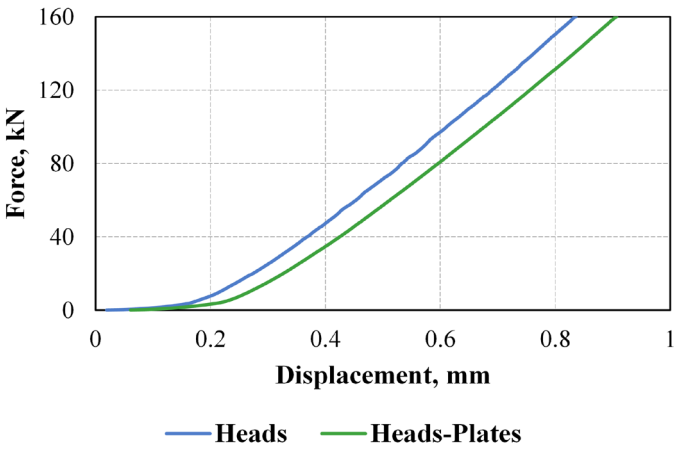

Fig. 8. Contact stiffness characteristics of the plate joint and the heads-plates system for the last unloading cycle

The resulting stiffness characteristics for the tested joint is shown in Fig. 9. The high steepness of this characteristics corresponds to the low roughness of the joined surfaces at the interface, due to the preparation of these surfaces by grinding.

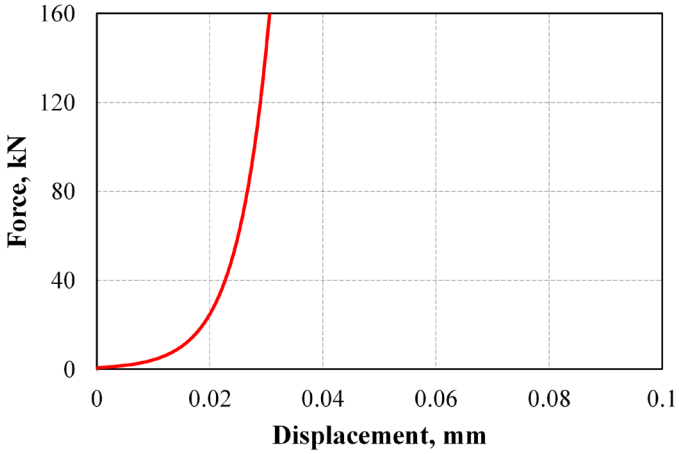

Fig. 9. Contact stiffness characteristics of the plate joint for the last unloading cycle

The course of the characteristics illustrated in Fig. 9 can be approximated by the following exponential function:

$$F = 0.7257 \cdot e^{176{,}45 \cdot u} \tag{1}$$

were F is the loading force and u is the relative displacement of the plates.

The coefficient of determination R^2 for the examined variables was 0.873, and was at an acceptable level.

4. Concluding remarks

The paper presents a methodology for determining the normal stiffness characteristics of a pair of plates joined in a multi-bolted connection. The developed characteristics is essential for contact modelling using the FEM. It makes it possible to take into account the actual stiffness of the joined elements and to introduce it independently for individual elements of the contact layer, e.g. in the form of non-linear springs. The presented methodology can be successfully applied to any other contact joint. The effects of this modelling will be presented in the second part of the paper. In the near future, it is also planned to perform similar tests aimed at determining the tangential stiffness characteristics for the contact joint under study.

This research did not receive any specific grant from funding agencies in the public, commercial, or not-for-profit sectors.

There is no conflict of interest.

REFERENCES

[1] L. Rakotondrainibe, J. Desai, P. Orval, G. Allaire, Eur. J. Mech. / A Solids **93**, 104499 (2022).

[2] P. Baranowski, K. Damaziak, J. Małachowski, Eksploat. Niezawodn. – Maint. Reliab. **15** (4), 337-342 (2013).

[3] E. Bachtiak-Radka, S. Dudzińska, D. Grochała, S. Berczyński, W. Olszak, Surf. Topogr.: Metrol. Prop. **5** (1), 015001 (2017).

[4] E. Bachtiak-Radka, S. Dudzińska, D. Grochała, S. Berczyński, Mechanik **92** (12), 778-780 (2019).

[5] J. Kluczyński, L. Śnieżek, K. Grzelak, A. Oziębło, K. Perkowski, J. Torzewski, I. Szachogłuchowicz, K. Gocman, M. Wachowski, B. Kania, Bull. Pol. Acad. Sci.: Tech. Sci. **68** (6), 1413-1424 (2020).

[6] A. Klimek, J. Kluczyński, J. Łuszczek, A. Bartnicki, K. Grzelak, M. Małek, Materials **15** (6), 1995 (2022).

[7] T. Smolnicki, D. Derlukiewicz, M. Stańco, Autom. Constr. **17** (3), 218-223 (2008).

[8] R. Walczak, J. Pawlicki, A. Zagórski, Arch. Metall. Mater. **61** (3), 1409-1416 (2016).

[9] P. Gutowski, M. Leus, Tribol. Int. **55**, 108-118 (2012).

[10] P. Wysmulski, H. Debski, Compos. Struct. **245**, 112356 (2020).

[11] P. Rozylo, H. Debski, Compos. Struct. **245**, 112388 (2020).

[12] P. Rozylo, Compos. Struct. **262**, 113598 (2021).

[13] B. Czajka, P. Różyło, Adv. Sci. Technol. Res. J. **16** (2), 216-224 (2022).

[14] R. Grzejda, K. Kwiatkowski, A. Parus, Int. Appl. Mech. **59** (3), 363-369 (2023).

[15] K. Konowalski, Adv. Manuf. Sci. Technol. **33** (3), 53-68 (2009).

[16] R. Buczkowski, M. Kleiber, Comput. Methods Appl. Mech. **195** (37-40), 5141-5161 (2006).

[17] S. Stupkiewicz, M. Lewandowski, J. Lengiewicz, Int. J. Solids Struct. **51** (23-24), 3931-3943 (2014).

[18] N.N. Balaji, W. Chen, M.R.W. Brake, Mech. Syst. Signal Process. **139**, 106615 (2020).

[19] A. Baltazar, S.I. Rokhlin, C. Pecorari, J. Mech. Phys. Solids **50** (7), 1397-1416 (2002).

[20] J.-Y. Kim, A. Baltazar, S.I. Rokhlin, J. Mech. Phys. Solids **52** (8), 1911-1934 (2004).

[21] S. Kucharski, G. Starzyński, Wear **440-441**, 203075 (2019).

[22] K. Grudziński, R. Kostek, Nonlinear Dynam. **50** (4), 809-815 (2007).

[23] R. Grzejda, Diagnostyka **15** (2), 61-64 (2014).

[24] R. Grzejda, J. Comput. Appl. Math. **393**, 113534 (2021).

[25] H. Xiao, Y. Sun, Int. J. Solids Struct. **155**, 240-247 (2018).

[26] P. Jaszak, Int. J. Press. Vessel. Pip. **176**, 103954 (2019).

[27] P. Jaszak, J. Skrzypacz, A. Borawski, R. Grzejda, Materials **15** (12), 4354 (2022).

[28] G. Shi, Y. Shi, Y. Wang, M.A. Bradford, Eng. Struct. **30** (10), 2677-2686 (2008).

[29] J. Cao, Z. Zhang, J. Mech. Sci. Technol. **33** (10), 4715-4725 (2019).

[30] H. Wang, Q. Wu, H. Qian, K. Han, F. Fan, Eng. Struct. **197**, 109407 (2019).

[31] M.M. Nia, S. Moradi, J. Constr. Steel Res. **187**, 106929 (2021).

[32] T. Sadowski, M. Kneć, P. Golewski, Int. J. Adhes. Adhes. **30** (5), 338-346 (2010).

[33] M. Chybiński, Ł. Polus, Structures **34**, 1942-1960 (2021).

[34] R. Grzejda, Eksploat. Niezawodn. – Maint. Reliab. **24** (2), 269-274 (2022).

[35] R. Grzejda, M. Warzecha, K. Urbanowicz, Lubricants **10** (5), 75 (2022).

[36] I.J. Drygala, M.A. Polak, J.M. Dulinska, Eng. Struct. **184**, 176-185 (2019).

[37] P. Wysmulski, Materials **15** (21), 7631 (2022).

[38] P. Wysmulski, Compos. Struct. **301**, 116184 (2022).

[39] P. Wysmulski, Compos. Struct. **305**, 116446 (2023).

[40] R. Grzejda, A. Parus, IEEE Access **9**, 47372-47379 (2021).

[41] R. Grzejda, A. Parus, FME Trans. **49** (3), 634-642 (2021).

[42] W.C. Oliver, G.M. Pharr, J. Mater. Res. **19** (1), 3-20 (2004).